Special Topic
Cutting-edge Carbon Utilization Technologies and Processes toward Carbon Neutral Industries

ISIJ International, Vol. 65 (2025), No. 13, pp. 2097–2104
https://doi.org/10.2355/isijinternational.ISIJINT-2025-186

Heat Transfer Enhancement by Forming Bridges among Reactive Particles in a Packed Bed Reactor of a Solid-gas Chemical Heat Storage System

Koichi NAKASO,[1)]* Kenji SHIMADA,[2)] Yasushi MINO[1,3)] and Kuniaki GOTOH[1)]

1) Faculty of Environmental, Life Natural Science and Technology, Okayama University, 3-1-1 Tsushima-naka, Kita-ku, Okayama, 700-8530 Japan.
2) Graduate School of Natural Science and Technology, Okayama University, 3-1-1 Tsushima-naka, Kita-ku, Okayama, 700-8530 Japan.
3) Faculty of Environmental Engineering, The University of Kitakyushu, 1-1 Hibikino, Wakamatsu-ku, Kitakyushu, Fukuoka, 808-0135 Japan.

(*Received June 10, 2025; Accepted October 17, 2025; Advance online published November 4, 2025; Published December 15, 2025*)

In this study, the enhancement of the thermal output of solid-gas chemical heat storage systems was investigated. Bridges made of high-thermal conductivity materials were formed among reactive particles by drying a slurry which contained graphite powder as a thermal additive and dispersant in a packed-bed reactor. First, the effect of the volume ratio of the dispersant on effective thermal conductivity was investigated. The optimum volume ratio of dispersant to graphite powder was determined. Furthermore, repetitive bridge formation increased the effective thermal conductivity. Based on these results, we investigated the thermal response of the energy-discharge process. Consequently, the temperature distribution in the radial direction of the reactor decreased owing to the formation of bridges. In addition, the thermal energy generated by the adsorption of water vapor onto the adsorbent was effectively transferred to the reactor wall. The thermal output was estimated based on the experimental results. The thermal output was increased by the formation of bridges.

KEY WORDS: chemical heat storage; packed bed; bridge among particles; heat transfer enhancement; effective energy utilization.

1. Introduction

Thermal energy storage (TES) is a key technology for effective utilization of energy to achieve a carbon-neutral society. There are three types of TES systems: sensible heat, latent heat, and chemical heat storage (CHS). CHS involves reversible thermochemical reactions. The advantage of CHS is that thermal energy is stored in reactive materials. This implies that there is no heat loss when energy is stored. Additionally, CHS, especially solid-gas CHS, works as a heat pump system. In other words, the temperature of the thermal discharge can be made higher than that of the thermal charge by selecting appropriate reaction conditions. Various temperature levels of waste heat are released from the steelmaking process. In particular, much exhaust heat below 200°C is released from the steelmaking process.[1)] Such low-temperature heat is difficult to utilize. Therefore, CHS can contribute to the utilization of thermal energy at temperatures below 200°C.

Figure 1 shows a schematic of a typical solid-gas CHS system. Solid reactive particles were packed into the reactor. A heat exchanger was placed in the packed bed reactor to supply and release chemical reaction heat. However, the heat transfer rate in a packed-bed reactor is typically low. This is because of its porous structure, which results in random contacts among the particles, and thermal resistance at each point of contact. Many attempts have been expended to enhance heat transfer in packed bed reactors. There are three main types of heat transfer enhancements; the first involves making composites with additives;[2,3)] the second involves the extension of the heat transfer area by the fins,[4,5)] and the third involves the direct contact between the heat transfer fluid and the reactive particles.[6–8)]

An example of fabricating composites with additives is the utilization of expanded graphite to increase the effective thermal conductivity. A high-volume fraction of the additive

* Corresponding author: E-mail: knakaso@okayama-u.ac.jp

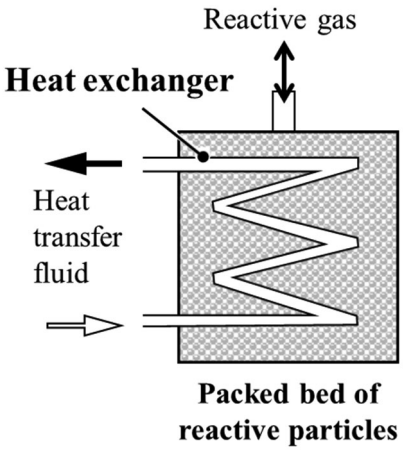

Fig. 1. Schematic of a typical chemical heat storage system.

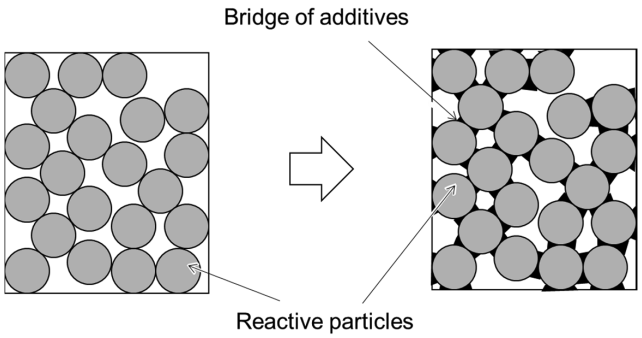

Fig. 2. Schematic illustration of bridge formations among reactive particles in the reactor.

is usually required to achieve high-effective thermal conductivity. Although the effective thermal conductivity of the packed bed increases, the pore volume fraction among the particles decreases. This implies that the flow of the reactive gas is blocked by the additive, and that the reaction is controlled by mass transfer, especially diffusion, rather than heat transfer.[2] Recently, Funayama *et al.* proposed a composite of reactive powders and porous silicon-impregnated silicon carbide.[9] This method successfully promoted the reaction without considering the limitations of mass transfer. However, applying it to reactors with complicated structures in practical CHS systems is difficult.

Many fins are typically required for heat transfer enhancement in packed bed reactors[4] because the contact area among the particles and fins is still small. In addition, the packing structure is influenced by the insertion of fins because the fins act as walls. This results in a reduction in the volume fraction of the reactive particles in the reactor, that is, in the energy density of the CHS system. In our previous studies, we evaluated the use of carbon fibers as thermal enhancers with various morphologies, including a carbon fiber brush[10] and a spiral fin around the heat transfer tube.[11] However, the contacts among the particles and the particles and wall/fin were insufficient and affected the overall heat transfer rate. To improve the contact between the reactive material and the fin, Kumita *et al.* prepared a porous aluminum oxide film on aluminum fins to absorb water vapor.[5] While this method considers both heat and mass transfer, it requires many fins with adsorbent film to increase energy storage density. Accordingly, heat transfer in a packed bed should be improved by considering mass transfer and energy storage density, simultaneously.

Considering the heat transfer phenomena in a packed bed, heat transfer was strongly influenced not only by the void, but also by the contact between the particles. Additionally, the contact between particles and the heat exchange surface is important for controlling the reaction and inputting/outputting thermal energy. Based on previous investigations, this study investigated the enhancement of the effective thermal conductivity of packed beds of reactive particles by forming bridges with a high-thermal-conductivity additive among the particles, as shown in **Fig. 2**. This study investigated the effects of bridges among reactive particles on the thermal output of zeolite/water solid-gas CHS. Assembling the additive around the contact points among the reactive particles increases the apparent heat transfer area among the particles; however, most of the pores in the packed bed remains in their original states. Thus, the effect of the thermal additive on the gas permeability of the packed bed can be reduced.

2. Experimental

2.1. Preparation of Bridges among Particles

Figure 3 shows a schematic of the procedure used for the formation of bridges among the particles. First, a thermal additive with a dispersant (as required) was mixed with water using a homogenizer. The slurry was then poured into a packed bed of reactive particles. Before bridge formation, the reactive particles were deactivated by water vapor to prevent reaction with water during bridge formation. After one hour, the slurry of the additive was drained from the packed bed reactor. At this point, liquid bridges around the contact point among the particles were formed by surface tension. Dry air was then introduced at the top of the reactor. The bridge formation procedure was performed twice to promote bridge formation. After the bridge was formed, the slurry mixture of the additives was poured into the packed bed again. After the slurry was drained, dry air was introduced into the packed bed. As a bridge can be formed after the reactive particles are packed into the reactor, it can be easily applied to practical CHS systems.

2.2. Estimation of Apparent Thermal Conductivity

The effective thermal conductivity of the packed bed was estimated as follows. First, the thermocouples were inserted into the packed bed before forming the bridge. Subsequently, a bridge was formed, as described in the previous section. Subsequently, the packed bed was placed in a thermostatic bath, and the wall temperature of the packed bed was changed from the room temperature T_0 to the preset temperature T_{set}. The changes in the temperature distributions in the packed bed were measured, as shown in **Fig. 4**. In this study, cylindrical vessel with an inner diameter of 37 mm and a height of 149 mm was used. Approximately 137 g of zeolite particles were packed in it. Graphite Powder (GP) and Vapor Grown Carbon Fiber (VGCF) were used as the thermal additive. As the dispersant, polyvinylpyrrolidone (PVP) was used. Properties of the materials used in this study is shown in **Table 1**.

To evaluate the experimental results, the heat conduction

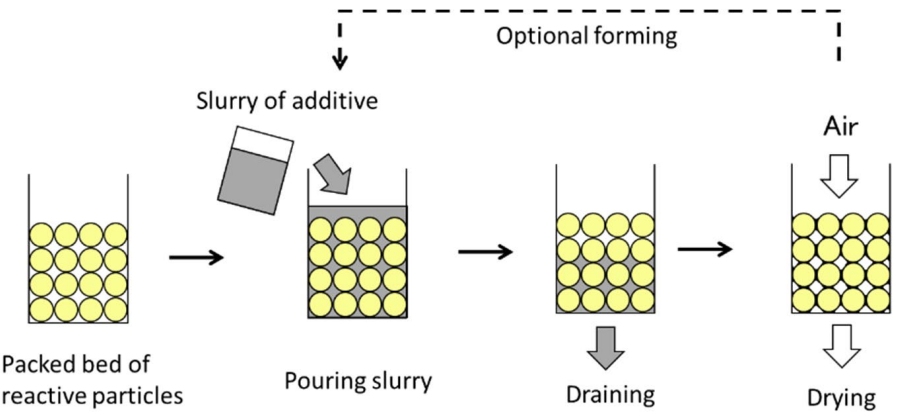

Fig. 3. Schematic illustration of heat transfer enhancement attributed to bridge formations among particles in packed bed. (Online version in color.)

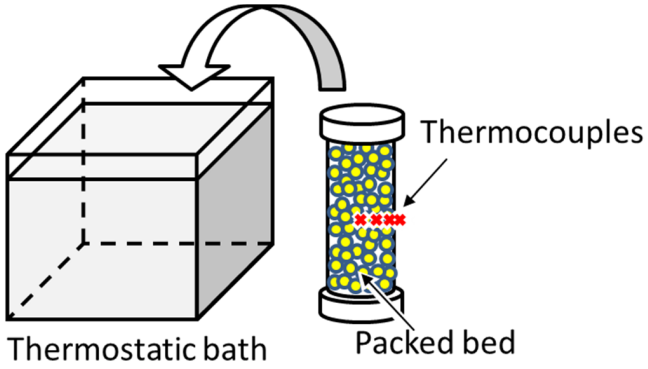

Fig. 4. Schematic of the experimental setup used for the estimation of the apparent effective thermal conductivity of the packed bed. (Online version in color.)

Table 1. Properties of the materials used in this study.

Zeolite (13X zeolite)	Average diameter: 4 mm
	Pore size: 10 Å
	Saturated water absorption: 0.27 kg-water/kg-zeolite
	Thermal conductivity: 0.15 W/(m·K)[7]
	Heat capacity: 700 J/kgK
Graphite Powder	Diameter: 5–11 μm
	Thermal conductivity: 100 W/(m·K)
	Heat capacity: 691 J/(kg·K)
	Density 2 100 kg/m^3
PVP	T_g = 150–180°C
	Heat capacity: 4 500 J/(kg·K)[12]
	Density 1 200 kg/m^3
VGCF	Theoretical thermal conductivity: 1 200 W/(m·K)[13,14]
	Heat capacity: 691 J/(kg·K)
	Density: 2 100 kg/m^3
Air	Thermal conductivity: 0.026 W/(m·K)
	Heat capacity: 1 006 J/(kg·K)

equations for the r-direction of the one-dimensional cylindrical coordinate system (see Eq. (1)) were solved by using the tentative thermal diffusivity α_m at the initial condition ($T = T_0$ at $t = 0$) and boundary condition ($dT/dr = 0$ at $r = 0$, and $T = T_{\text{exp inside}}$ at $r = R$).

$$\frac{\partial T}{\partial t} = \alpha_m \frac{1}{r}\frac{\partial}{\partial r}\left(r\frac{\partial T}{\partial r}\right) \quad \text{..... (1)}$$

Subsequently, the sum-of-the-squares of the differences between the experimental and numerical results with various thermal diffusivities was calculated. When the sum-of-the-squares of the differences between the experimental and numerical results was the smallest, the thermal diffusivity was determined as the sample's apparent thermal diffusivity. The apparent thermal conductivity was obtained by considering the apparent density and heat capacity calculated using the volume fraction of the components under the preparation conditions.

2.3. Effects of Bridges on the Thermal Performance of CHS

Figure 5 shows a schematic of the experimental apparatus. The CHS system consisted of a packed-bed reactor, a water reservoir for water vapor, and a vacuum pump. Zeolite particles were used as the CHS material in the packed bed reactor. Its average diameter was approximately 4.0 mm. Four thermocouples were placed in the reactor to quantify the temperature distribution along the radial direction. The reactor was then placed in an oil bath. During the TES (charging) process, the packed bed was vacuumed and its outer parts were heated at ~140–150°C for 6.5 h. During the thermal release (discharging) process, water vapor from the evaporator was introduced into the packed-bed reactor. The heating temperature of the evaporator was set at 120°C. To avoid condensation of water vapor, tubes were kept at 100°C by the heating cables and the temperature controllers. The adsorption heat was transferred from the outer wall of the reactor to silicone oil as a heat transfer fluid in the oil bath. The oil-bath's temperature was maintained at 100°C. In this study, the effect of a thermal additive bridge on the performance of a zeolite-water CHS was investigated, especially for the thermal discharge process. The effect of the bridge on the thermal output was studied. For the heat resistance of PVP for CHS system use is also studied and described in the appendix.

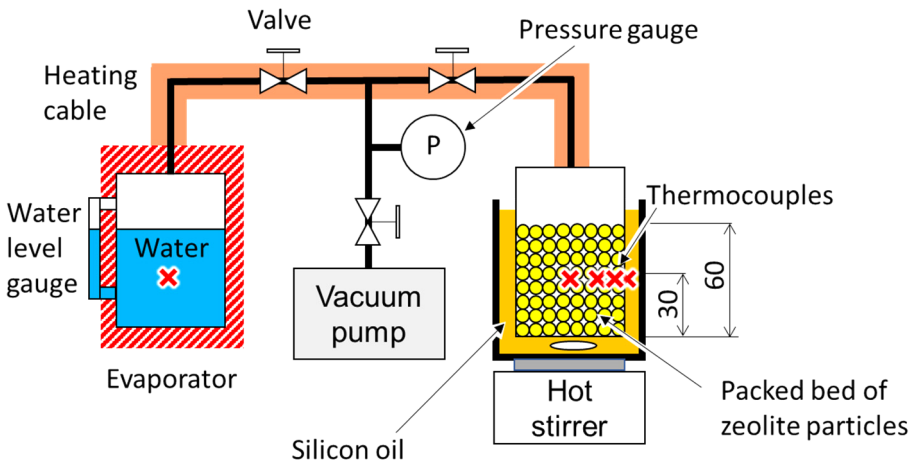

Fig. 5. Schematic of experimental apparatus for chemical heat storage. (Online version in color.)

3. Results and Discussion

3.1. Effects of Dispersant on the Effective Thermal Conductivity

Figure 6 shows a comparison between the estimated and experimental local temperatures in the packed bed. The markers indicate the measured local temperatures. The lines are the calculated local temperatures corresponding to the measured points in the packed bed, assuming a thermal diffusivity of 2.05×10^{-7} m^2/s. Figure 6 shows that the temporal variations of local temperatures could be estimated by assuming $\alpha_m = 2.05 \times 10^{-7}$ m^2/s. To obtain the apparent thermal conductivity k_{app} from the thermal diffusivity α_m, the apparent density ρ_{app}, and heat capacity $C_{p,app}$ are required. These were estimated using the volume fraction of the components (*i.e.*, particle, fluid, and bridge). Based on the Eq. (2), $k_{app} = 0.152$ W/(m·K).

$$\alpha_m = \frac{k_{app}}{\rho_{app} C_{p,app}} \quad \text{..... (2)}$$

Using the same procedure, the effect of the dispersant on effective thermal conductivity was studied. **Figure 7** summarizes these results. The GP volume fraction was fixed at 0.875 vol%. As shown in the figure, there is a maximum value of the apparent thermal conductivity. At lower volume fractions, the apparent thermal conductivity increased as a function of the volume fraction of the dispersant. In other words, the dispersion of graphite powder was insufficient at lower dispersant fractions. As the dispersant ratio increases, the dispersion of GP increases. At higher volume fractions, the apparent thermal conductivity decreases. This can be attributed to the decrease in the ratio of GP to the total solid volume owing to the increase in the volume fraction of the dispersant. Figure 7 also plots the volume fractions of GP and PVP in the packed bed. These values were calculated based on the mass of the slurry remaining in the packed bed after draining, taking into account the volume fractions of GP and PVP in the prepared slurry. As seen in the figure, the apparent thermal conductivity did not correspond to an increase in the volume of bridge material (GP + PVP). This suggests that PVP does not significantly improve thermal conductivity. Moreover, a double formation was carried out for the cases of PVP of 3.5 vol%. The results are summarized in **Table 2**. As seen in the table, the apparent thermal

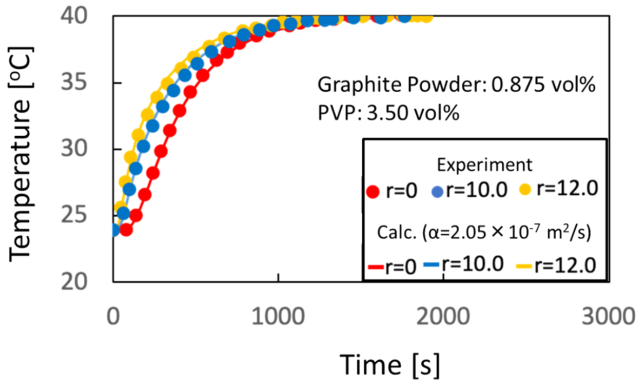

Fig. 6. Example of comparisons between estimated and experimental results. (Online version in color.)

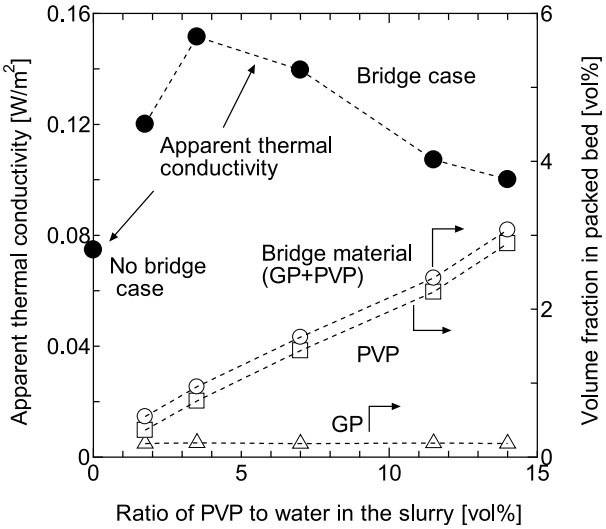

Fig. 7. Effect of ratio of dispersant on the apparent thermal conductivity of packed bed.

conductivity increased from 0.152 to 0.174 W/(m·K).

Figure 8 shows photographs of the particles with a bridge of additives in the packed bed. To capture these photographs, the particles in the upper part of the packed bed were removed by manually crashing the bridges. Because the color of the zeolite particles is white, the black parts indicate staining with the additive. The black circles on the surfaces of the zeolite particles denote the bridges. Based

Table 2. Summary of apparent thermal conductivities.

	Volume fraction of additive	Volume fraction of PVP	Void fraction	Apparent thermal conductivity W/(m·K)
Single forming (GP)	0.002	0.008	0.396	0.152
Double forming (GP)	0.003	0.011	0.391	0.174
Single forming (VGCF)	0.003	0.014	0.388	0.171

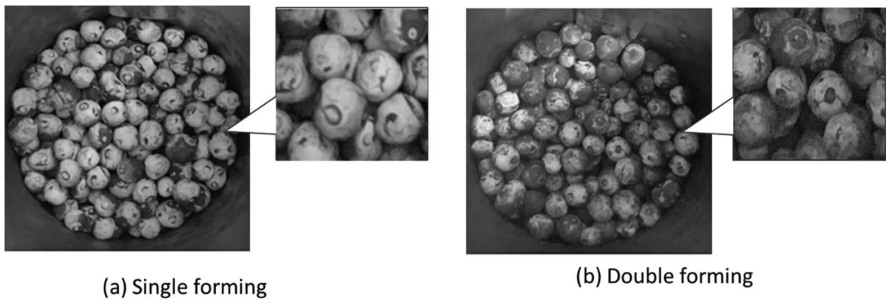

Fig. 8. Photographs of particles with additive bridges.

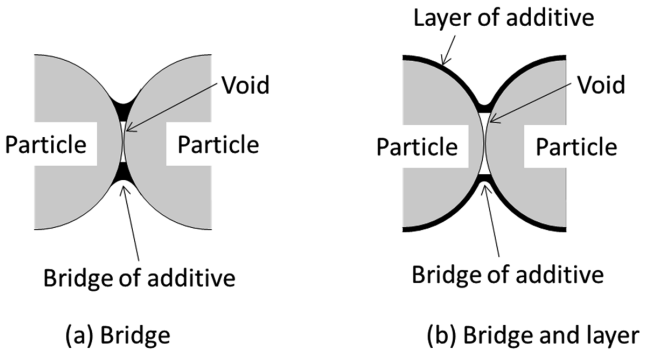

Fig. 9. Schematic of structures of the bridges of the additive among particles.

on these observations, the corresponding structures formed among the particles are shown in **Fig. 9**. As indicated, the bridge appears to have a hollow structure. This type of hollow structure can be observed in drying phenomena, such as granule production by a spray dryer.[15] Although there is a void in the bridge, the zeolite particles are bound to the bridge of the additive. In the double-forming case, some of the particles were covered with an additive. If all the surfaces of the zeolite were covered with the additive, heat transfer would be promoted. However, the reactivity decreased simultaneously. This issue will be discussed in later sections.

Here, the heat transfer enhancement with VGCF, a kind of carbon nanotube is also investigated. The theoretical thermal conductivity of VGCF is 1 200 W/(m·K). However, it exhibits anisotropic thermal characteristic. While the thermal conductivity in the longitudinal direction is extremely high, the thermal conductivity in the transverse direction is similar to that of general carbon materials. In the experiment, the volume fractions of PVP and VGCF were the same as in the optimal GP condition (*i.e.*, 3.5 vol% PVP and 0.875 vol% VGCF). The result is also shown in Table 2. Contrary to expectations, the apparent thermal conductivity with VGCF was slightly higher than that with GP. This implies VGCF were randomly packed in the bridge between particles. In order to utilize VGCF's potential as a thermal additive, it is essential to control its orientation in the bridge. From another angle, GP exhibits similar performance to VGCF, which were randomly packed. In this study, GP is selected as the thermal additive for chemical heat storage because of its environmental impact and cost.

3.2. Theoretical Study on the Effect of Additive on the Apparent Thermal Conductivity

The effect of the additive on apparent thermal conductivity was theoretically investigated. To estimate the apparent thermal conductivity, Kunii-Smith's equation[16] is used. When the radiation heat transfer can be ignored, the equation can be expressed as follows:

$$k_{app} = \varepsilon k_f + \frac{1-\varepsilon}{\phi\left(\frac{1}{k_f}\right)+\frac{2}{3}\left(\frac{1}{k_S}\right)} \quad \text{..... (3)}$$

where, k, ε, ϕ are thermal conductivity, void fraction, and the parameter defined by Eqs. (4)–(7), respectively. The subscripts app, f, and s expresses apparent, fluid, and solid, respectively.

$$\phi = \phi_2 + \left(\phi_1 - \phi_2\right)\frac{\varepsilon - 0.26}{0.216}\left(0.476 > \varepsilon > 0.26\right) \quad \text{..... (4)}$$

$$\phi = \phi_1(\varepsilon > 0.476) \quad \text{..... (5)}$$

$$\phi = \phi_2(\varepsilon < 0.26) \quad \text{..... (6)}$$

$$\phi_{1,2} = \frac{\frac{1}{2}\left(\frac{K-1}{K}\right)^2 \sin^2\phi_0}{\ln\left\{K-\left(K-1\right)\cos\phi_0\right\}-\frac{K-1}{K}\left(1-\cos\phi_0\right)} - \frac{2}{3}\left(\frac{1}{K}\right) \quad \text{..... (7)}$$

$$K = \frac{k_s}{k_f} \quad \text{..... (8)}$$

Table 3. Estimated apparent thermal conductivities.

Component	Apparent thermal conductivity W/(m·K)	Total void fraction
Main particle: zeolite Void: Air	0.069	0.40
Main particle: GP Void: Air	0.450	0.40
Main particle: zeolite Void: Air → GPpacked bed	0.280	0.16
Main particle: zeolite Void: Air → zeolite packed bed	0.106	0.16

The results are summarized in **Table 3**. As the reference data, the apparent thermal conductivity of zeolite packed bed is estimated to 0.069 W/(m·K). For the estimation zeolite packed bed, parameters are set to k_s = 0.15 W/(m·K), k_f = 0.026 W/(m·K), and ε = 0.40, respectively. Moreover, the apparent thermal conductivity of GP packed bed is estimated to 0.45 W/(m·K). In this case parameters were set by k_s =100 W/(m·K), k_f = 0.026 W/(m·K), and ε = 0.40, respectively.

Next, the replacement of voids with a packed bed of additives or storage particles is studied. In general, additives such as expanded graphite are applied to a packed bed by filling the voids between the particles. Assuming the packing structure is independent of particle size, the effect of an additive filling the void on apparent thermal conductivity is estimated by replacing the void (fluid region) in a packed bed of large particles with a packed bed of smaller particles. The apparent thermal conductivities were estimated using Eqs. (3) through (8), changing the thermal conductivity of the fluid region from 0.026 W/(m·K) (air) to 0.45 W/(m·K) (GP packed bed) or 0.069 W/(m·K) (zeolite packed bed). The results showed apparent thermal conductivities of 0.28 W/(m·K) and 0.106 W/(m·K), respectively. These results demonstrate that replacing the voids with a packed bed can improve the apparent thermal conductivity. However, the void fraction of the composite packed bed decreases from 0.4 to 0.16 (= 0.4^2). Additionally, the pore size of void in the packed bed decreases. These facts result in decreased permeability of reactive gas through the packed bed, *i.e.*, inhibition of the solid-gas reaction. This trade-off relationship would be improved by the bridge formation method presented in this study. Since the present method concentrates the additive only on the particle contact areas, the reduction in voids is minimal. For example, the slurry condition of 3.5 vol% PVP and 0.875 vol% GP results in a maximum apparent thermal conductivity of 0.152 W/(m·K), as shown in Fig. 7. In this case, its void fraction was approximately 0.396. Moreover, for the double-forming case, the apparent thermal conductivity was 0.174 W/(m·K) and the void fraction was approximately 0.391.

3.3. Application of the Present Method to the CHS System

The proposed heat transfer enhancement method was applied to a CHS system, as shown in Fig. 5. In this study, the cases of PVP of 3.5 vol% and GP of 0.875 vol% were fixed, which led to the maximum apparent thermal conductivity, as discussed in the previous section. The no-bridge, single-, and double-forming cases were compared. In this study, the discharge process was investigated. **Figure 10** shows the temporal variations in the local temperature of the packed bed reactor. In the no-bridge case, the center temperature increased up to 190°C, and then gradually decreased to the temperature of the heat transfer fluid. Although the temperature at r = 9 mm exhibited a similar tendency to that of the center temperature, the maximum temperature was 175°C. The inner- and outer-wall temperatures increased only during the early stages of the reaction. However, in the bridge cases, the temperature difference in the radial direction decreased. Moreover, the temperature inside the packed bed decreased more rapidly. These tendencies were emphasized by changing from single- to double-forming.

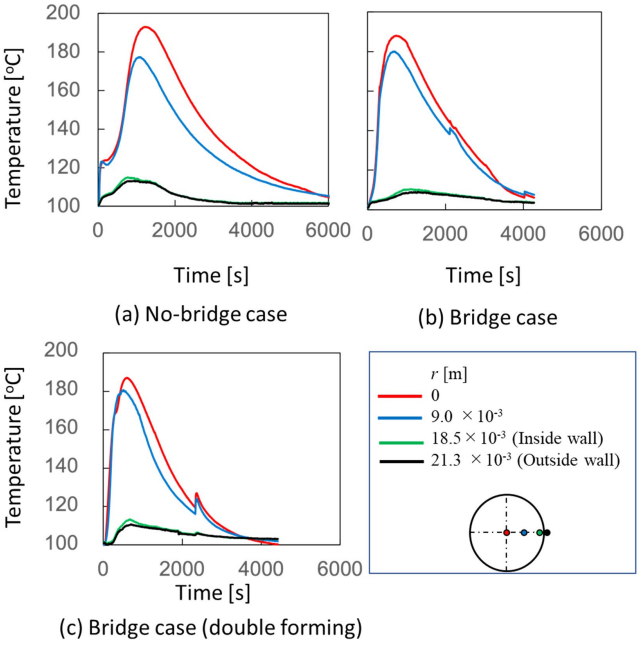

Fig. 10. Temporal variation of temperature in the packed bed reactor in chemical heat storage conditions during the discharging process. (Online version in color.)

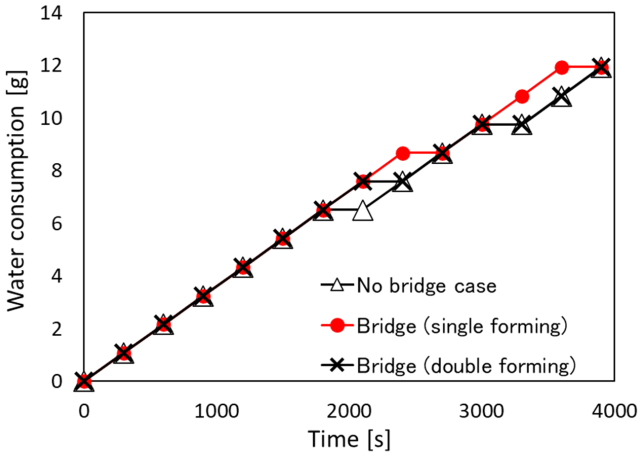

Fig. 11. Water consumption in the reservoir. (Online version in color.)

Figure 11 shows the temporal variations in water consumption in the reservoir under various conditions. The water mass was calculated by measuring the liquid level. During the discharge process, water vapor filled the interior

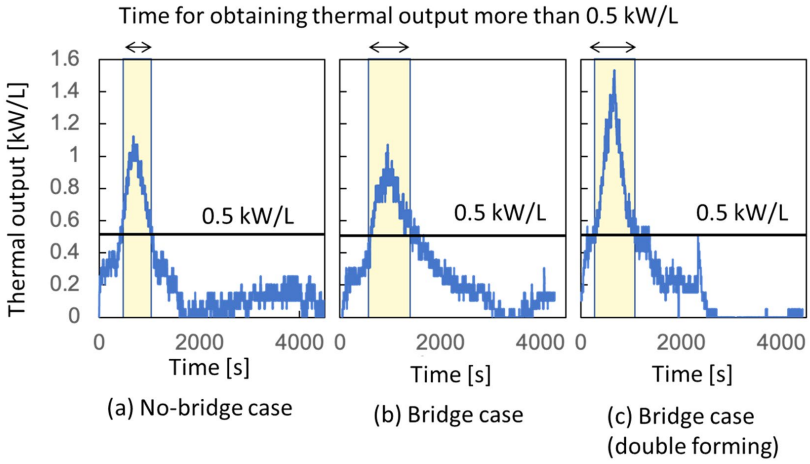

Fig. 12. Temporal variation of thermal output of the chemical heat storage system. (Online version in color.)

of the apparatus, including the reservoir, reactor, and tube. When water vapor was adsorbed by the zeolite, evaporation occurred to compensate for the decrease in water vapor due to adsorption. Therefore, the water consumption corresponds to the progress of adsorption. Figure 11 shows that the water consumption in the bridge case is slightly faster than that in the no-bridge case. Furthermore, the total water consumption is similar under all conditions. This suggests that the effects of the additive on water adsorption on the zeolite surface can be ignored, even though the additive partially covered the surface.

3.4. Effects of the Bridge on the Thermal Output of the Chemical Heat Storage System

Based on the experimental results, the thermal output was calculated based on the following equation:[17)]

$$Q = k_w A_{lm} \frac{\left(T_{w,inside} - T_{w,outside}\right)}{\Delta r} \quad \text{..... (9)}$$

where Q, k_w, A_{lm}, $T_{w,inside}$, $T_{w,outside}$, Δr are thermal output, thermal conductivity of the reactor wall, logarithmic mean area for heat transfer, temperature of the inner reactor wall, temperature of the outer reactor wall, and the thickness of the reactor wall, respectively. A_{lm} can be expressed as follows,

$$A_{lm} = \frac{A_{w,outside} - A_{w,inside}}{\ln \dfrac{A_{w,outside}}{A_{w,inside}}} = \frac{2\pi\left(R_{w,outside} - R_{w,inside}\right)L}{\ln \dfrac{2\pi R_{w,outside} L}{2\pi R_{w,inside} L}} = \frac{2\pi L dr}{\ln \dfrac{R_{w,outside}}{R_{w,inside}}} \quad \text{.... (10)}$$

where L is the height of the packed bed of the reactive particles. The thermal output was estimated by assuming that the temperature in the vertical direction (z-direction) was uniform. **Figure 12** shows the temporal variations in the thermal outputs under various conditions. As shown in the figure, the thermal output was increased by forming a bridge, particularly in the double-forming case. Herein, the target heat transfer rate per unit reactor volume of 0.5 kW/L was considered for the practical utilization of the energy storage system. The time required to achieve thermal outputs > 0.5 kW/L increased in the bridge case. **Table 4** summarizes the calculated thermal outputs. The thermal output increased owing to the bridge formations. In particular, the thermal output of the double-forming case was higher than that of the single-forming case.

Table 4. Thermal output calculated based on the experimental results.

	No bridge	Bridge case (Single forming)	Bridge case (Double forming)
Averaged thermal output per unit volume of the reactor [kW/L]	0.211	0.281	0.484

4. Summary

To improve the thermal output of a chemical heat storage unit, the heat transfer enhancement by forming bridges among particles was investigated. It was found that the temperature distribution decreased owing to the formation of bridges among the particles. It was also found that the adsorption heat was effectively transferred to the heat transfer fluid by forming a bridge. The thermal output was also increased owing to the formation of bridges. These tendencies were emphasized by changing from single- to double-forming. A higher concentration of the additive in the bridge would be necessary to achieve higher performance.

Statement for Conflict of Interest

The authors declare no conflicts of interest related to this research.

Acknowledgments

This study was partially supported by the Hosokawa Powder Technology Foundation and JSPS KAKENHI (Grant Number JP16K06972). The authors thank Ms. Misato Torigoe for performing the experiments.

Appendix. Heat Resistance of PVP for CHS System Use

This study uses PVP to disperse GP. However, in order to apply it to the CHS system, the heat resistance of PVP must first be studied. Thus, a heat resistance test was conducted that involved directly heating the bridges formed between

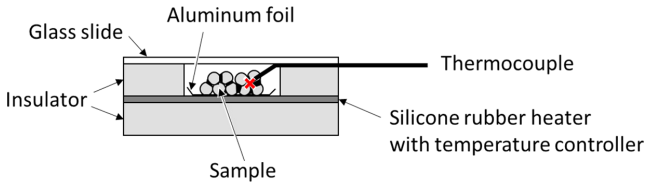

(a) Schematic of the experimental apparatus

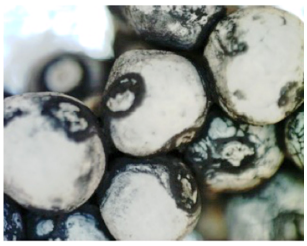

(b) Photograph of particles with bridges before heating (24.8°C)

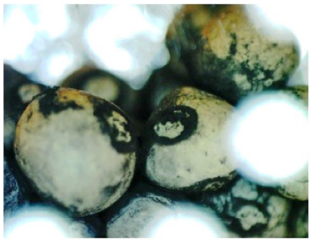

(c) Photograph of particles with bridges at the maximum temperature (176°C)

Fig. A1. The experimental apparatus and results of the heat resistance test. (Online version in color.)

particles. The bridges formed among particles (3.5 vol% PVP and 0.875 vol% GP) are heated using a heater and observed as shown in **Fig. A1**(a). Figures A1(b) and A1(c) show the photographs of the bridges among particles before heating and at the maximum temperature (176°C), respectively. As can be seen, the bridges maintained their structure without collapsing at the 176°C. PVP does not have a clear melting point but rather a glass transition point between 150 and 180°C. This indicates softening rather than melting. CHS materials are known to undergo repeated expansion and contraction through reversible reactions. Additionally, concerns have been raised that vibrations during transportation may damage the packing structure when it is used for heat transport. Although the durability of these materials requires further discussion, the softening effect caused by the glass transition could greatly enhance the durability of CHS devices.

REFERENCES

1) NEDO and TherMAT: Survey on waste heat in industrial fields, Published online 2019:13. https://www.nedo.go.jp/news/press/AA5_101074.html (Aug., 2025).
2) K. Wang, J.Y. Wu, R.Z. Wang and L.W. Wang: *Int. J. Refrigeration*, **29** (2006), 199. https://doi.org/10.1016/j.ijrefrig.2005.06.004
3) M. Zamengo, J. Ryu and Y. Kato: *Appl. Therm. Eng.*, **64** (2014), 339. https://doi.org/10.1016/j.applthermaleng.2013.12.036
4) M. Groll: *Heat Recover. Syst. CHP*, **13** (1993), 341. https://doi.org/10.1016/0890-4332(93)90059-5
5) M. Kumita, M. Meiwa, K. Watanabe and A. Kodama: *Appl. Therm. Eng.*, **50** (2014), 1564. https://doi.org/10.1016/j.applthermaleng.2012.04.010
6) B. Xue, Y. Iwama, Y. Tanaka, K. Nakashima, A.T. Wijayanta, K. Nakaso and J. Fukai: *Exp. Therm. Fluid Sci.*, **46** (2013), 54. https://doi.org/10.1016/j.expthermflusci.2012.11.020
7) B. Xue, K. Tahara, K. Nakashima, A. Noda, E. Oktariani, A.T. Wijayanta, K. Nakaso and J. Fukai: *J. Chem. Eng. Jpn*, **45** (2012), 408. https://doi.org/10.1252/jcej.12we016
8) K. Nakaso, Y. Tanaka, S. Eshima, S. Kobayashi and J. Fukai: *ISIJ Int.*, **55** (2015), 448. https://doi.org/10.2355/isijinternational.55.448
9) S. Funayama, M. Schmidt, K. Mochizuki, M. Linder, H. Takasu and Y. Kato: *Appl. Therm. Eng.*, **220** (2023), 119675. https://doi.org/10.1016/j.applthermaleng.2022.119675
10) K. Nakaso, A. Yoshimuram, Y. Kitazato, R. Shigenaga and J. Fukai: *J. Chem. Eng. Jpn*, **40** (2007), 1056. https://doi.org/10.1252/jcej.06WE246
11) K. Nakaso, H. Kang, T. Aoki and J. Fukai: *Kagaku Kogaku Ronbunshu*, **35** (2009), 511 (in Japanese). https://doi.org/10.1252/kakoronbunshu.35.511
12) K. Ishikiriyama, K. Kondo, Y. Miyazaki, Y. Sasada, K. Sawada, R. Endo, N. Man, M. Nakano and Y. Nakazawa: *Thermochim. Acta*, **722** (2023), 179456. https://doi.org/10.1016/j.tca.2023.179456
13) Y. Nagao: *Kobunshi*, **53** (2004), 793. https://doi.org/10.1295/kobunshi.53.793
14) K. Nakaso, T. Aoki, T. Tada and J. Fukai: *J. the Soc. Powder Technol., Jpn*, **46** (3) (2009), 162 (in Japanese). https://doi.org/10.4164/sptj.46.162
15) K. Nakaso, D. Yamashita, Y. Aoyama, Y. Mino and K. Gotoh: *Earozoru Kenkyu*, **40**(2) (2025), 99 (in Japanese). https://doi.org/10.11203/jar.40.99
16) D. Kunii: Netsuteki Tanisosa Jou, Maruzen, (1976), 138 (in Japanese).
17) F.P. Incopera, D.P. Dewitt, T.L. Bergman and A.S. Lavine: Introduction to Heat Transfer, 5th ed., John Wiley & Sons, (2007), 97. ISBN 0-471-51728-3